THESIS FOR THE DEGREE OF LICENTIATE OF ENGINEERING

Towards structural design optimisation of railway crossings

Henrik Vilhelmson

Department of Mechanics and Maritime Sciences
Division of Dynamics
Chalmers University of Technology
Gothenburg, Sweden, 2024

Towards structural design optimisation of railway crossings

Henrik Vilhelmson

Copyright © 2024 Henrik Vilhelmson
All rights reserved.

Technical report no 2024:04

Department of Mechanics and Maritime Sciences
Division of Dynamics
Chalmers University of Technology
SE-412 96 Gothenburg, Sweden
Phone: +46 (0)31 772 1000
www.chalmers.se

Printed by Chalmers Reproservice
Gothenburg, Sweden, August 2024

Abstract

Railway switches and crossings (S&C, turnouts) connect different track sections and create a robust railway network by allowing trains to change tracks. While this provides valuable flexibility to the railway network, the flexibility comes at a cost. The maintenance, production and environmental costs for one turnout are significantly higher than the corresponding costs per kilometer of plain track due to the complex wheel–rail interaction and severe loading it has to endure during its lifetime. In one of the critical parts of the turnout, the crossing panel, high dynamic wheel–rail contact forces occur each time a train passes, even in the through route. In this thesis, the dynamics of the passage through the crossing panel is simulated and the structural loading is evaluated. The aim is to improve the long-term performance of the crossing panel by reducing the magnitude of the dynamic wheel–rail contact forces, while simultaneously reducing the material use to decrease environmental footprint and life cycle cost.

To this end, an extensive simulation model of a crossing panel is developed that enables extraction of the structural loading of each component. Based on measured data from a comprehensively instrumented demonstrator turnout, it is calibrated and validated using a calibration method that is developed in the thesis. The calibration is accomplished by tuning the parameters that are related to the support conditions of the crossing, such as sleeper support stiffness and sleeper–ballast voiding. After the calibration, very good correlation between simulation and measurements is achieved. In preparation for an optimisation of the crossing panel, which utilises the calibrated model and allows for significant design changes, structural requirements are proposed. These include dynamic load scenarios established from field measurements and load limits for the components within the crossing panel. In future work, the intention is to use the calibrated model together with the structural requirements in a structural design optimisation of the crossing panel.

Keywords: Switch & crossing, S&C, turnout, multi-body simulations, MBS, model calibration, dynamic load scenarios, dynamic vehicle–track interaction, wheel–rail contact forces, structural optimisation, structural requirements.

Preface and Acknowledgements

The work presented in this thesis was completed at the Division of Dynamics at the Department of Mechanics and Maritime Sciences, Chalmers University of Technology, between August 2022 and September 2024. It was performed as part of the activities within the National Centre of Excellence in Railway Mechanics CHARMEC (CHAlmers Railway MEChanics, www.charmec.chalmers.se) within the project TS23 – "Optimisation of crossing panel design for improved long-term performance". This work was supported by the Horizon 2020 Framework Programme in the Shift2Rail projects In2Track2 and In2Track3 [grant numbers 826255 and 101012456], and the Europe's Rail project R2DATO [grant number 101102001]. The computations and data handling were enabled by resources provided by the National Academic Infrastructure for Supercomputing in Sweden (NAISS) and the Swedish National Infrastructure for Computing (SNIC) at C3SE partially funded by the Swedish Research Council through grant agreements nos. 2022-06725 and 2018-05973.

I want to thank my supervisors Docent Björn Pålsson and Professor Jens Nielsen from whom I have learnt a lot in such a short time. You always take the time to thoroughly understand, question, discuss and improve my work. I am very thankful for the humble, egalitarian and motivating research environment that you, together with the colleagues at CHARMEC and the Division of Dynamics, provide. An extra thanks to Jim Brouzoulis for making my teaching hours even more enjoyable.

In addition to my academic collaborators, I would like to thank Mr Thomas Titze and Mr Uwe Ossberger at voestalpine Railway Systems GmbH, Dr Rikard Bolmsvik at Heidelberg Materials Precast Abetong AB and, Dr Martin Li and Mr Jan-Erik Meyer at Trafikverket (Swedish Transport Administration) who have provided me with important industrial knowledge and perspective.

Till mina föräldrar "Mona & Lasse", tack för ert ändlösa stöd och för att ni alltid lyssnar på vilka problem jag har hittat på den här veckan. Jag vill även nämna mina bröder Oskar och Joakim, nu är era namn förevigade i vetenskapslitteraturen.

List of Publications

This thesis includes the following publications:

Paper A
Björn A. Pålsson, Henrik Vilhelmson, Uwe Ossberger, Michael Sehner, Marko D.G. Milošević, Harald Loy and Jens C.O. Nielsen, Dynamic vehicle–track interaction and loading in a railway crossing panel – Calibration of a structural track model to comprehensive field measurements, *Vehicle System Dynamics*, 1–27, 2024. 10.1080/00423114.2024.2305289.

Paper B
Henrik Vilhelmson, Björn A. Pålsson, Jens C.O. Nielsen, Uwe Ossberger, Michael Sehner and Harald Loy, Dynamic vehicle–track interaction and structural loading in a crossing panel – Calibration and assessment of a model with a 3D representation of the crossing rail, *Vehicle System Dynamics* 1–23, 2024. 10.1080/00423114.2024.2319275.

Paper C
Henrik Vilhelmson, Björn A. Pålsson and Jens C.O. Nielsen, Assessment of structural requirements for crossing panel design using dynamic load case scenarios, *Proceedings of the Sixth International Conference on Railway Technology* (Railways 2024), 1–5 September 2024, Prague, Czech Republic, 16 pp.

Contents

Part I

Extended summary

CHAPTER 1

Introduction

1.1 Background and motivation

The railway turnout (Switch & Crossing, S&C) is often categorised as a "hungry asset" inducing high maintenance costs [1]. The density of S&Cs in most railway networks is estimated to be about one per km of track, which equates to over 300 000 units within the networks of the EU27 countries [2]. The cost of maintenance of an S&C unit is believed to be equivalent to that of about 0.3 km of plain line track. In 2015, the average yearly investment and maintenance cost for 10 812 S&Cs installed in the Swedish network was estimated to be in the order of 590 million SEK [3]. In addition to the high costs of installation and maintenance, an S&C contains significantly more concrete and steel than plain line track per km, leading to higher CO_2 emissions.

The existing rail discontinuities in a turnout lead to high dynamic wheel–rail contact forces, in particular in the crossing panel [4]. This is one of the main causes of the increased maintenance cost and the need for a reinforced structure. Failures associated with S&Cs account for 25–30% of all infrastructure failures on the European railways [5]. Based on data from the Swedish network collected between 2014 and 2020, failures in the crossing panel were relatively few in number but led to one of the highest average traffic delays per failure of almost 350 minutes [6]. This may be compared to the switch panel, where the average delay per failure was around 150 minutes although failures were more common. The number of trains affected by the crossing failures was also one of the highest recorded in the study. Given these factors, there are strong economic and environmental incentives for optimisation of the crossing panel.

1.2 Aim of research

The work in this thesis is an effort towards a structural optimisation of the railway crossing panel design to improve long-term performance and reduce environmental impact and life cycle cost. To facilitate such an optimisation, the aim of the thesis has been to develop, firstly, a validated simulation model that accurately can capture the structural loading in the relevant components within the crossing panel. Secondly, based on a combination of simulations, field measurements and existing regulations, dynamic load case scenarios and structural requirements to be used as constraints in the optimisation have been formulated. The performed work is split into three papers.

- Dynamic vehicle–track interaction and loading in a railway crossing panel – Calibration of a structural track model to comprehensive field measurements (**Paper A**).
- Dynamic vehicle–track interaction and structural loading in a crossing panel – Calibration and assessment of a model with a 3D representation of the crossing rail (**Paper B**).
- Assessment of structural requirements for crossing panel design using dynamic load case scenarios (**Paper C**).

The following parts are planned in the future of the project:

- Optimisation of the elastic pads, sleepers and crossing rail within the crossing panel for improved long-term performance and reduced environmental impact and life cycle cost.

CHAPTER 2

The crossing panel

The turnout is an essential component in railway networks as it allows trains to switch between tracks. In the crossing panel (the part of the turnout that is illustrated in Figure 2.1), the wheel flanges must pass through the rail. To allow for this, the rail is split into a crossing nose and two wing rails (together often referred to as the crossing rail or frog, see Figure 2.2) divided by a gap creating two possible routes for the train, a through route and a diverging route. The switch rails can be manoeuvred to select which route the passing vehicle should take. While this provides valuable flexibility to the railway network, the flexibility comes at a cost as the gap and the variation in cross-section of the rail profiles in the S&C result in higher rail (and wheel) degradation rates than in plain line track. Traffic in the facing direction (move) goes from the wing rail to the crossing nose, while traffic in the trailing move goes in the opposite direction.

S&Cs can be installed on slab track or ballasted track. This research is focused on ballasted track. The sleepers are fastened to the rails either by a direct or an indirect (including a baseplate) fixation, and an elastic pad is placed between the rail and the sleeper. In most modern S&Cs, an elastic under sleeper pad (USP) is mounted under the sleeper to reduce the contact pressure between the sleeper and ballast. Sleepers used in turnouts have a slightly different shape compared to sleepers in plain line track and also vary in length along the turnout. In this thesis, the focus is on the fixed crossing type, where the crossing nose is fixed in place, in contrast to the swing-nose crossing type where the crossing nose can be moved depending on route similar to the switch rails.

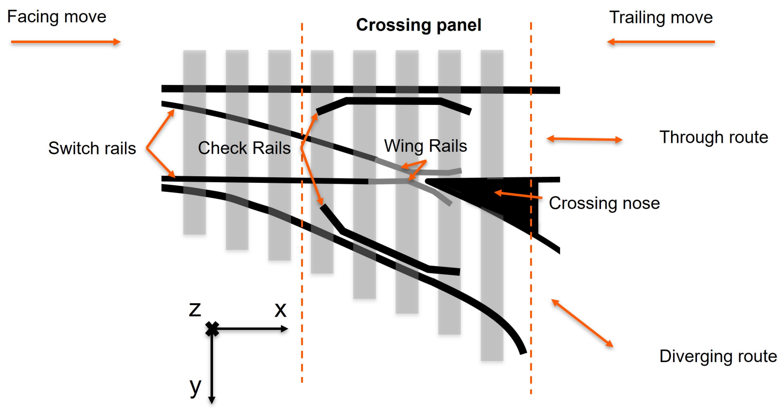

Figure 2.1: Illustration of a crossing panel within a turnout.

2.1 Wheel–rail contact in the crossing panel

When a wheel passes through the crossing in the facing move, the wheel–rail contact point will move towards the outside of the wheel profile as the wing rail deviates laterally (states A and B in Figure 2.3). For a typical conical wheel profile, as the wheel travels in the longitudinal direction along the wing rail, the rolling radius will decrease and the wheel will move downwards. To counteract this downward movement, the wing rail is sometimes elevated in modern designs. The rolling radius difference induces a yawing motion of the wheelset towards the crossing, but due to the check rail, the lateral motion of the wheelset is restrained and wheel flange interference contact with the crossing nose is prevented. When the wheel transitions from the wing rail to the crossing nose, a very short duration of two-point contact commonly occurs (state C). As the contacts have different rolling radii, a relative motion occurs in the contacts that causes severe wear during the transition. In addition to

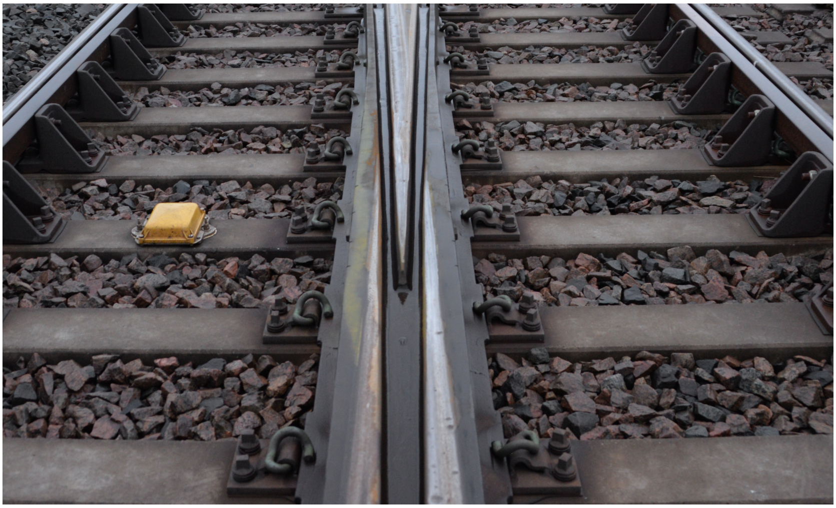

Figure 2.2: A crossing rail (two wing rails and a crossing nose) within a crossing panel.

this, the conicity of the wheel in combination with the variation in rail geometry along the crossing results in a wheel–rail excitation that is characterised by a dip in the vertical wheel trajectory. This leads to wheel–rail impact loading (state D) that increases in magnitude with speed and crossing angle [4], which accelerates the deterioration of both the crossing panel and wheel. As the deterioration increases, the contact geometry changes, and with worn contact conditions impact loads can increase drastically [7]. In field measurements, impact loads over 400 kN have been recorded even at lower axle loads and speeds [8].

2.2 Damage modes in the crossing panel

There are several reviews of damage mechanisms in turnouts [2, 9–11]. In [9, 10], the focus is on rail damage, while in [2, 11] damage is presented for each component. Common damage modes on the crossing rail running surface are wear, rolling contact fatigue (RCF) related effects such as head checks, spalling/shelling, cracks and squats, and plastic deformation. All of these damage modes are related to high wheel–rail contact forces. To rectify surface

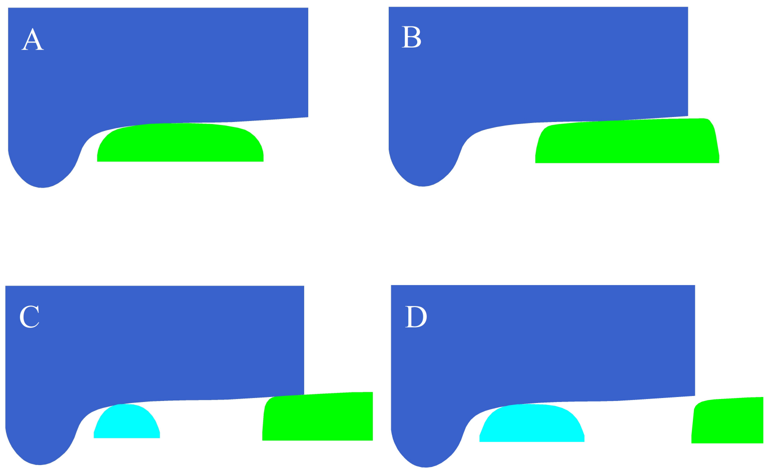

Figure 2.3: Different states of wheel–rail contact (A–D) during the crossing panel transition. The wheel profile in blue, the wing rail in green and the crossing nose in cyan.

damages such as those mentioned above, rail maintenance such as welding, grinding/deburring, repair/build-up welding or in severe cases, replacement is required.

Damage to sleepers is more rare as there is no contact damage from the wheel and is mostly related to cracks due to high bending moments. In [11], where statistical data for each type of failure within the turnout is reported, it is clear that the sleeper is very underrepresented. However, a change in sleeper support conditions caused by differential settlement of the ballast that may create voids between the sleeper and ballast is more common. This is often corrected by tamping, although it is more difficult to tamp in a turnout. Field measurements have indicated the presence of ballast voids or hanging sleepers within S&Cs, as in **Paper A** [12–16]. Additionally, the ballast stones may be crushed under loading, compromising the quality of the ballast bed, which may require replacement of the ballast stones.

Based on the data initially categorised in [11], and further refined in [17] to failures occurring specifically in the crossing panel, the most common damage modes in the crossing panel have been identified to be voids between sleeper

(a) **(b)** **(c)**

Figure 2.4: Examples of damage modes on the crossing rail: (a) plastic deformation, (b) wear, (c) RCF (spalling). Pictures are courtesy of voestalpine Railway Systems GmbH.

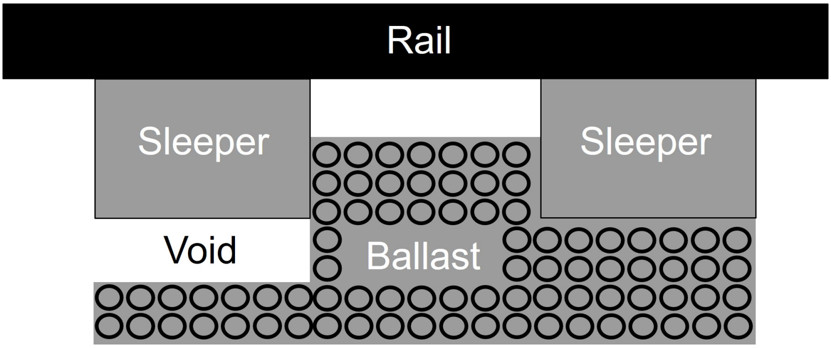

Figure 2.5: Illustration of a ballast void.

and ballast (60.9% of reported failures in the crossing panel), cracked/broken casting (19.3%) and wear (14.9%). The remaining 5.1% are other failures related to rails, ballast or fixations. In the Failure Modes and Effects Analysis (FMEA) carried out in [17], each failure mode is given a Risk Priority Number (RPN). This number is based on the probability of the failure occurring, the sensitivity of the failure (how sensitive the train network is to the particular failure) and the difficulty of detecting the failure. The RPN determines the overall risk of the failure mode. The result of the analysis concluded that the highest risk is a cracked/broken casting (RPN 60), followed by ballast voiding (30) and rail wear (24). In [18], the results from a similar study also showed that cracking and wear of the crossing rail are the most critical damage modes.

Note that the study in [18] did not consider sleeper voiding as a failure mode and therefore it was not listed.

2.3 Optimisation of the crossing panel

To reduce the deterioration and improve long-term performance, the optimisation of S&Cs has been a topic of interest in recent years, with some of the research involving the crossing panel in particular [17, 19–28]. Generally, one component (crossing rail, sleeper or elastic pads) at a time has been considered and the main focus has been on reducing the vertical wheel–rail contact forces. In [19], the running surface geometry of the crossing rail was optimised to minimise the maximum Hertzian wheel–rail contact pressure for a representative set of wheel profiles and to ensure that all transitions occur within the specified transition zone. A similar study was performed in [20]. In [24], also by modifying the running surface, the performance of the crossing was improved by reducing the normal wheel–rail contact pressure and wear index. Two different materials for the crossing rail are compared regarding plastic deformation and wear in [27].

The most common approach focuses on optimising the elastic pad stiffnesses to improve load distribution and decrease deterioration related to some of the most common failure modes. Examples considered in the literature include wear, RCF, differential settlement and fatigue of the track components studied in [17], wheel–rail contact forces and rail seat loads in [22], and loads on the ballast in [23, 28]. In the European Research Programme Shift2Rail, an S&C demonstrator was developed and built [25, 26]. This demonstrator has, for example, a variation in rail pad and USP stiffnesses along the turnout together with widened sleeper bases near the sleeper ends. General conclusions from these listed studies are that varying USP and rail pad stiffness in the turnout is beneficial, softer pads reduce ballast settlement, wheel–rail forces, wear, rail pad forces and sleeper acceleration, but increase bending stresses in the rail foot. The research is summarised in Table 2.1, highlighting which design variables were covered in each reference.

Among the studies mentioned, only the Shift2Rail reports included the sleepers as a design variable. Most studies have assumed that as the magnitude of the wheel–rail contact force remains the same or is reduced, then so is the structural loading. However, in the continuation of this thesis, a

Author	Elastic pads	Sleepers	Crossing rail
Grossoni [17]	x		
Pålsson [19]			x
Nicklisch [21]	x		x
Lau [22]	x		
Wan/Markine [23, 24]	x		x
Shift2Rail [25, 26]	x	x	x
Skrypnyk [27]			x
Li [28]	x		

Table 2.1: Published articles concerning optimisation of the crossing panel, displaying which design variables were studied by each author.

structural optimisation allowing for significant changes in the design of each component is planned, making requirements on a limit of the allowed increase in structural loading necessary. Another very important aspect that often has been ignored in previous optimisation works is the sleeper support conditions. These support conditions are not only very difficult to quantify but also change over time due to differential settlement in the ballast and subgrade. These aspects increase the complexity of the optimisation problem, but by considering the change in structural loading the possibility to further improve the performance of the crossing panel by also optimising the size, topology or shape of each component is introduced.

CHAPTER 3

Method

3.1 Simulation model in short

The simulation model is a representation of the 60E1-500-1:12 (60E1 rails, radius of 500m and a crossing angle of 1:12) Shift2Rail demonstrator turnout. It is an extension of the models created and further refined in previous projects within CHARMEC [29–31], and it is created in the multibody simulation software Simpack. The model consists of 37 sleeper bays, linear bushings for the rail fastenings and bi-linear bushings for the ballast and subgrade to allow for potentially voided sleepers. The rails are implemented as substructures created from FE-models using Craig-Bampton reduction [32]. The stock rails are made up of beam elements, while the crossing rail is represented by beam elements (**Paper A**) or 3D solid elements (**Paper B**). The vehicle model includes one bogie based on the Manchester benchmark vehicle [33]. The 3D version of the model is shown in Figure 3.1. Laser-scanned rail and wheel geometries from the field are used. The initial conditions of the vehicle and track models are determined by evaluating the static equilibrium for the vehicle–track system before the start of each time-domain simulation. The model is described in more detail in **Paper A** and **Paper B**.

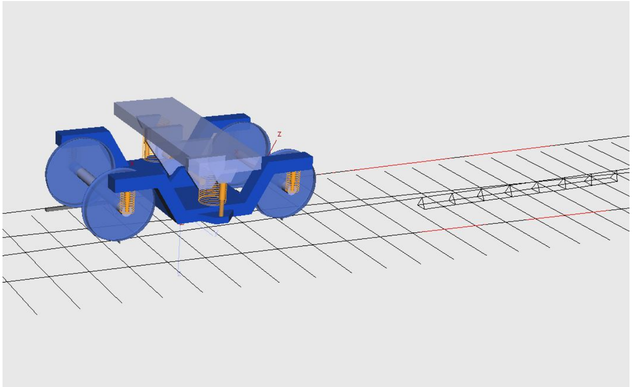

Figure 3.1: The simulation model in Simpack. From **Paper B**.

3.2 Calibration of the simulation model

From the output of the simulation model, the structural loading of the crossing panel (crossing rail, sleeper and ballast) is extracted in a post-processing step. Based on the comprehensive measurement data from the S&C demonstrator installed in the European research programme Shift2Rail, the model is calibrated and validated in **Paper A** and **Paper B**. The measurements include, sleeper–ballast contact pressures, strains for sleeper and crossing rail, and accelerations for sleepers and crossing rail. All sensors included in the calibration and their groups can be seen in Figure 3.2.

An example of results from the nominal (before calibration) models is presented in Figure 3.3. When comparing the outputs of the beam and 3D models, the most notable difference is the significant increase in longitudinal bending stress in some positions on the ribs of the bottom of the crossing rail (that are not considered in the beam model) due to stress concentration factors, see Figure 3.4. In both models, the ballast is parameterised using six parameters to potentially introduce voids under the sleeper below the crossing nose and two parameters to control support stiffness, one uniform ballast (subgrade included) stiffness scaling parameter for the entire track model and one for the rail fastening stiffness.

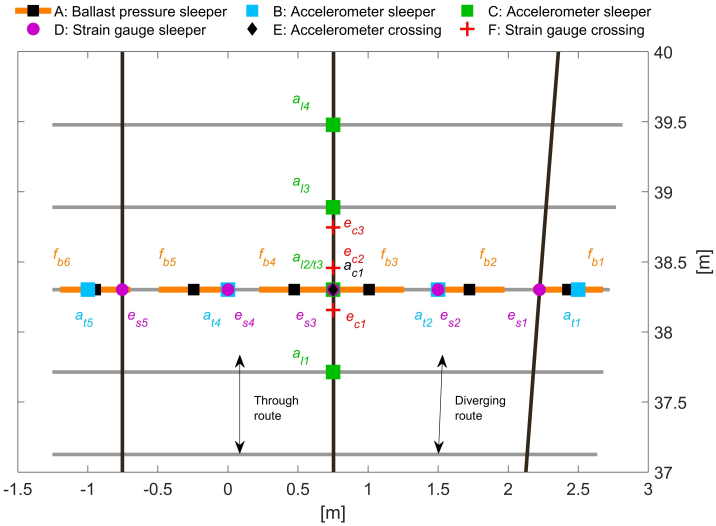

Figure 3.2: Sensor groups, locations and labels in the instrumented crossing panel. From **Paper A**.

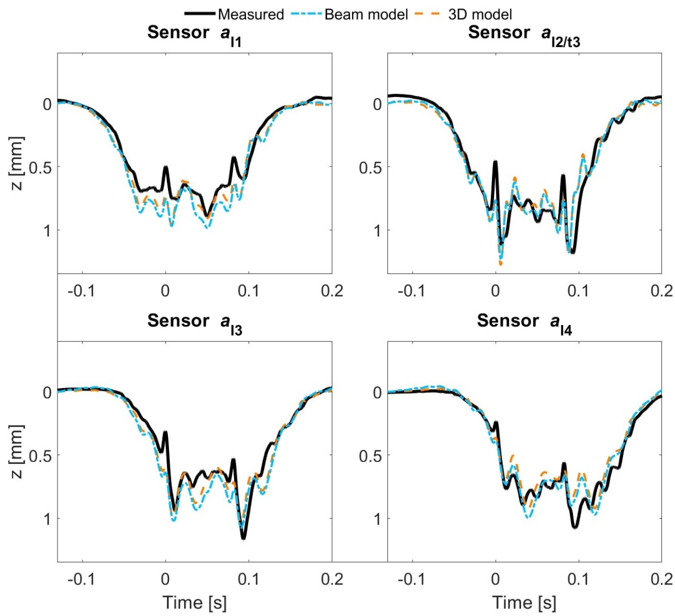

Figure 3.3: Group C results for beam and 3D models with nominal parameter settings, and comparison with measured data. From **Paper B**.

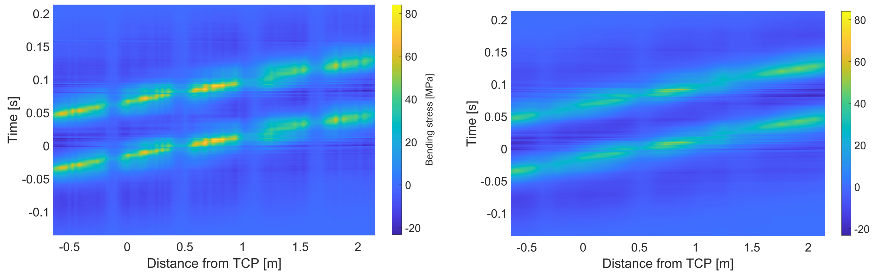

(a) **(b)**

Figure 3.4: Time history of longitudinal rail bending stress evaluated for positions along the crossing panel (relative to the distance from the theoretical crossing point). The selected lateral coordinate on the crossing is aligned with the most loaded rib on the bottom surface of the crossing. a) 3D model b) beam model. From **Paper B**.

To evaluate the quality of calibration, an objective function based on the root mean square (RMS) value of the difference between the measured and simulated signals has been introduced. The different sensor groups had the potential to have different weighting factors in the objective function.

The calibration process contained several steps. To set appropriate weighting factors and parameter intervals, it was initiated with a sensitivity study of the simulation model from parameter sets generated using Latin hypercube sampling (LHS) [34]. A response surface was created from LHS-generated simulation runs within the new parameter intervals using a polyharmonic spline. The response surface was then evaluated using Monte Carlo validation, and the results showed a maximum deviation between simulation and measurement below 5.5% and a mean deviation below 0.9%. A gradient-based optimisation algorithm was then applied to the response surface to find the optimal parameter set. The process is summarised as a flowchart in Figure 3.5.

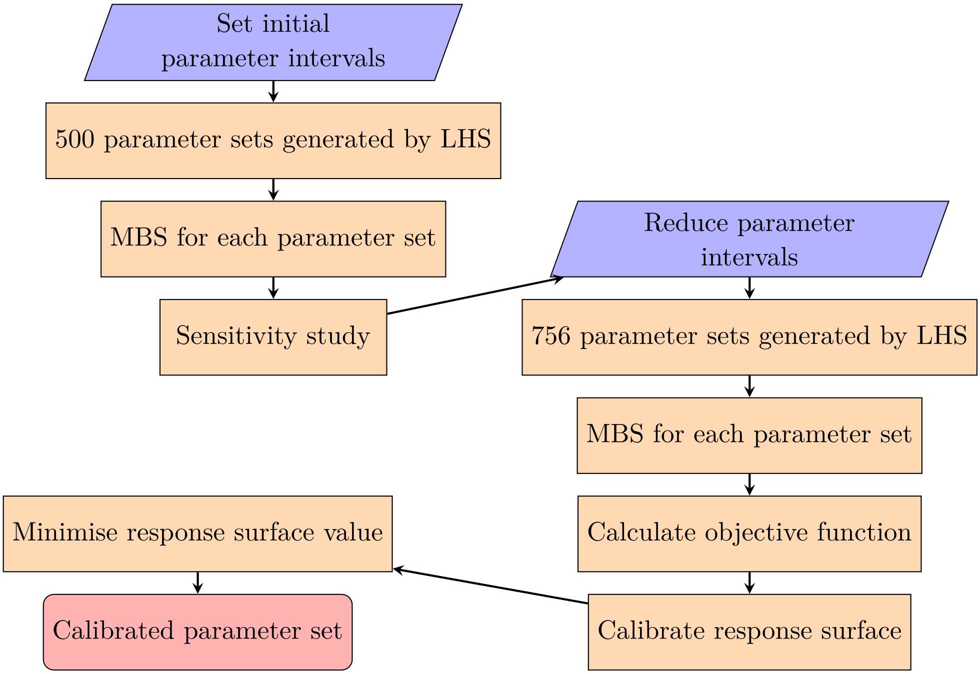

Figure 3.5: Calibration flowchart. From **Paper B**.

The results of the calibration show increased rail fastening and ballast stiffnesses, while still within the values given in literature. The calibrated void distribution indicates that the voids are primarily located underneath the crossing rail.

3.3 Structural requirements

In **Paper C**, structural requirements for an S&C are proposed. For the S&Cs used in the Swedish railway network, standardised traffic load scenarios (combinations of train speeds and axle loads) that the turnout is required to withstand have been specified in [35]. After simulations of all these scenarios using the model described above, the most severe has been concluded to be the scenario with a train speed of 60 km/h and an axle load of 30 tonnes.

As a change in design can lead to an increase in the structural loading, the load limits for the most relevant components need to be determined. Limits for crossing rail, sleepers and ballast have been determined and are presented in Table 3.1. However, in the upcoming optimisation, in addition to the hard load limit on the ballast, a penalty function based on the relative increase of settlement compared to a reference case will be implemented. Further, it should be noted that the specified sleeper limit corresponds to the crack initiation limit and not a fatigue limit as the one given for the crossing rail.

Component	Stress limit [MPa]	Limit category
Crossing rail	173.3	Fatigue limit
Sleeper	10.6	Crack initiation limit
Ballast	0.3	Load bearing limit

Table 3.1: Component load limits for use in the optimisation. From **Paper C**.

In [7], six crossing panels were studied in-situ. Based on the measured data from each crossing panel, a simulation model was calibrated to determine the sleeper support conditions. The calibration indicated between one and three hanging sleepers with voids in the interval 0.55 – 2 mm for three of the crossing panels. In particular, one crossing panel in very poor condition was calibrated to have four hanging sleepers with a 5 mm void. Based on these observations, representative sleeper–support conditions can be determined and used in the optimisation.

CHAPTER 4

Future work

An optimisation to reduce the environmental impact and life cycle cost of the crossing panel is planned in future work. Design variables such as elastic pad stiffnesses and the dimensions of crossing rails and sleepers will be considered.

Based on the developed and calibrated model, it is argued that the potential impact of innovative designs for sleepers and crossing rail can be evaluated. It is possible to study how these designs can improve the long-term performance of the crossing panel.

4.1 Example of optimisation problem

The design variables of the optimisation problem are collected in a vector denoted as the vector $\mathbf{u}$. It includes:

- c_H - Crossing rail height
- c_W - Crossing rail width
- s_H - Sleeper height
- s_W - Sleeper width
- h_1 - Rail fastening stiffness

- h_2 - Under sleeper pad stiffness

A potential optimisation problem has the goal of reducing the environmental impact from the lifespan of a crossing panel. One way to do this is by minimising the total CO_2 emissions per crossing panel while maintaining the structural integrity. The optimisation problem can then be formulated as:

$$\begin{aligned} \min_{\mathbf{u}} \quad & m_s \mathrm{CO}_{2,\mathrm{eq,s}} + m_c \mathrm{CO}_{2,\mathrm{eq,c}} + p(\mathbf{u}) \\ \text{s.t.} \quad & \sigma_{\mathrm{c}} < g_{\mathrm{crossing}} \\ & \sigma_{\mathrm{s}} < g_{\mathrm{sleeper}} \\ & \sigma_{\mathrm{b}} < g_{\mathrm{ballast}} \end{aligned} \tag{4.1}$$

where m_s and m_s are the total mass for the sleepers and the crossing rail, respectively, while $\mathrm{CO}_{2,\mathrm{eq,c}}$ and $\mathrm{CO}_{2,\mathrm{eq,s}}$ are the equivalent carbon dioxide emissions ($\mathrm{CO}_{2\mathrm{eq}}$) per kg crossing rail and sleeper, respectively. The constraints g_{crossing}, g_{sleeper}, g_{ballast} are the specified load limits for the components, see Table 3.1. The equivalent CO_2 per kg component is determined based on the public environmental product declarations provided by the producer. The $p(\mathbf{u})$ is a penalty function proportional to a ballast settlement model. It is defined as

$$p(\mathbf{u}) = \begin{cases} \gamma((\frac{\sigma_b}{\sigma_{ref}})^{\beta} - 1) & \text{if } \sigma_b > \sigma_{ref} \\ 0 & \text{otherwise} \end{cases} \tag{4.2}$$

where σ_b is the maximum pressure on the ballast bed, σ_{ref} is the maximum pressure on the ballast bed for a reference case, and γ is a weighting factor. The exponent β determines the expected exponential increase in settlement with increasing ballast pressure. This parameter is difficult to determine and varies depending on the conditions in the field. Here β is set to 2.8 based on the calibration performed in [36].

CHAPTER 5

Summary of appended papers

This chapter provides a summary of the appended papers.

Paper A
Björn A. Pålsson, Henrik Vilhelmson, Uwe Ossberger, Michael Sehner, Marko D.G. Milošević, Harald Loy and Jens C.O. Nielsen, Dynamic vehicle–track interaction and loading in a railway crossing panel – Calibration of a structural track model to comprehensive field measurements, *Vehicle System Dynamics*, 1–27, 2024. 10.1080/00423114.2024.2305289.

This paper presents a finite element model of a railway crossing panel for use in multibody simulations (MBS). The model is calibrated and validated to measurement data from a comprehensively instrumented S&C demonstrator installed in the Austrian railway network as a part of the European research programme Shift2Rail. The validation concerns the capability of the model to capture the structural response of the crossing panel under traffic loading after calibration of physical track parameters to realistic values. The structural response is measured in the form of rail and sleeper displacements and strains and sleeper–ballast contact forces. It is shown that the developed model can represent the measured track responses well but that it was necessary to account for a varying sleeper–ballast gap distribution along the crossing transition sleeper to obtain good agreement, especially for the sleeper–ballast pressure.

> **Paper B**
> Henrik Vilhelmson, Björn A. Pålsson, Jens C.O. Nielsen, Uwe Ossberger, Michael Sehner and Harald Loy, Dynamic vehicle–track interaction and structural loading in a crossing panel – Calibration and assessment of a model with a 3D representation of the crossing rail, *Vehicle System Dynamics* 1–23, 2024. 10.1080/00423114.2024.2319275.

The MBS model from **Paper A** is extended to include a crossing rail represented by 3D solid elements. The applied procedure for the calibration and critical assessment of the crossing model is described in detail. In a comparative study, it is shown that the 3D model and the more conventional beam model (from **Paper A**) of the crossing rail lead to similar calibration results and good agreement with the measured data. The 3D model allows for the extraction of stress concentrations in the crossing rail but has an increased computational time of about 30% compared to the beam model.

> **Paper C**
> Henrik Vilhelmson, Björn A. Pålsson and Jens C.O. Nielsen, Assessment of structural requirements for crossing panel design using dynamic load case scenarios, *Proceedings of the Sixth International Conference on Railway Technology* (Railways 2024), 1–5 September 2024, Prague, Czech Republic, 16 pp.

Structural requirements for railway crossing panel design are proposed. These include dynamic load scenarios established from field measurements, and structural load limits for the crossing rail, sleepers and maximum allowed vertical contact stress on the ballast surface. The applied load scenarios are established by combining measured data from scanned hollow worn wheel profiles, scanned crossing rail geometries, and sleeper–ballast voids extracted by calibrating a track model to measured sleeper accelerations. Using the two track models developed in **Paper A** and **Paper B**, the structural load limits are challenged using the dynamic load scenarios. The study shows that the highest dynamic wheel–rail contact loading is achieved for a geometry where a nominal crossing rail geometry (virgin rail profile) is combined with a hollow worn wheel profile. The study provides an understanding of what field conditions the crossing panel could be subjected to before the loading exceeds the load limits of the components.

References

[1] Pålsson BA and Bezin Y. Editorial for S&C benchmark special issue. *Vehicle System Dynamics*, 61(3):639–643, 2023.

[2] Capacity4Rail. Deliverable D1.3.1, Operational failure modes of switches and crossings. 2015. 61 pp.

[3] Trafikverket (The Swedish Transport Administration). Detaljering av underhållskostnader på sidospår samt analys av användandet av icke avgiftsbelagt sidospår (Specification of maintenance costs in side tracks and analysis of the use of non-tolled side tracks, in Swedish). 2015. 81 pp.

[4] Jenkins HH, Stephenson JE, Clayton GA, Morland GW, and Lyon D. The effect of track and vehicle parameters on wheel/rail vertical dynamic forces. *Railway Engineering Journal*, 3(1):2–16, 1974.

[5] In2Rail. D02.7 - Self inspecting adjusting S&C systems concept design report, 2015. 50 pp.

[6] Ait Ali A, Odolinski K, Pålsson BA, and Torstensson P. Evaluating the mix of maintenance activities on railway crossings with respect to life-cycle costs. *European Journal of Transport and Infrastructure Research*, 24(1):1–29, Jun. 2024.

[7] Milošević MDG, Pålsson BA, Nissen A, Nielsen JCO, and Johansson H. Condition monitoring of railway crossing geometry via measured and simulated track responses. *Sensors*, 22(3):1012, 2022.

[8] Shih JY, Weston P, Entezami M, and Roberts C. Dynamic characteristics of a switch and crossing on the west coast main line in the UK. *Railway Engineering Science*, 30(2):183–203, 2022.

[9] Dahlberg T, Ekh M, Nielsen JCO, and Sällström JH. State-of-the-art study on railway turnouts: Dynamics and damage. Research Report 2004:8, Department of Applied Mechanics, Chalmers University of Technology, Göteborg, 2004. 50 pp.

[10] Grossoni I, Hughes P, Bezin Y, Bevan A, and Jaiswal J. Observed failures at railway turnouts: Failure analysis, possible causes and links to current and future research. *Engineering Failure Analysis*, 119:104987, 2021.

[11] Hassankiadeh SJ. Failure analysis of railway switches and crossings for the purpose of preventive maintenance. Royal Institute of Technology (KTH) Stockholm, Sweden. 2011. 79 pp.

[12] Liu X and Markine VL. Train hunting related fast degradation of a railway crossing – Condition monitoring and numerical verification. *Sensors*, 20(8):2278, 2020.

[13] Le Pen L, Watson G, Hudson A, and Powrie W. Behaviour of under sleeper pads at switches and crossings – Field measurements. *Proceedings of the Institution of Mechanical Engineers, Part F: Journal of Rail and Rapid Transit*, 232(4):1049–1063, 2018.

[14] Wheeler LN, Take WA, Hoult NA, and Le H. Use of fiber optic sensing to measure distributed rail strains and determine rail seat forces under a moving train. *Canadian Geotechnical Journal*, 56(1):1–13, 2019.

[15] Sysyn M, Nabochenko O, and Kovalchuk V. Experimental investigation of the dynamic behavior of railway track with sleeper voids. *Railway Engineering Science*, 28(1):290–304, 2020.

[16] Shih JY, Weston P, Entezami M, Roberts C, and O'Callaghan M. Experiences using MEMS accelerometers on railway bearers at switches and crossings to obtain displacement—Awkward situations. *Infrastructures*, 9(6):91, 2024.

[17] Grossoni I, Bezin Y, and Neves S. Optimisation of support stiffness at railway crossings. *Vehicle System Dynamics*, 56:1–25, 11 2017.

[18] In2Track. D2.1 Research into enhanced tracks, switches and structures, 2018. 191 pp.

[19] Pålsson BA. Optimisation of railway crossing geometry considering a representative set of wheel profiles. *Vehicle System Dynamics*, 53(2):274–301, 2015.

[20] Lee J, de O Lima A, Dersch MS, and Edwards JR. Optimisation of turnout frog profile geometry using revenue service wheel profiles. *Vehicle System Dynamics*, 62(5):1142–1159, 2024.

[21] Nicklisch D, Kassa E, Nielsen JCO, Ekh M, and Iwnicki S. Geometry and stiffness optimization for switches and crossings, and simulation of material degradation. *Proceedings of the Institution of Mechanical Engineers, Part F: Journal of Rail and Rapid Transit*, 224(4):279–292, 2010.

[22] Lau A. Numerical simulation of switch and crossing towards an optimized turnout design. Norwegian University of Science and Technology, Trondheim, Norway, PhD thesis, 2018.

[23] Wan C, Markine VL, and Shevtsov I. Optimisation of the elastic track properties of turnout crossings. *Proceedings of the Institution of Mechanical Engineers, Part F: Journal of Rail and Rapid Transit*, 230(2):360–373, 2016.

[24] Markine VL and Wan C. Performance optimised geometry of railway crossings: Design and implementation. *International Journal of Railway Technology*, 5:1–25, 2016.

[25] In2Track. D2.2 Enhanced S&C Whole System Analysis, Design and Virtual Validation, 2020. 411 pp.

[26] In2Track2. D01.2 - Research into enhanced track and switch and crossing system 2, 2021. 122 pp.

[27] Skrypnyk R, Ekh M, Nielsen JCO, and Pålsson BA. Prediction of plastic deformation and wear in railway crossings – Comparing the performance of two rail steel grades. *Wear*, 428-429:302–314, 2019.

[28] Li X, Nielsen JCO, and Torstensson PT. Simulation of wheel–rail impact load and sleeper–ballast contact pressure in railway crossings using a

Green's function approach. *Journal of Sound and Vibration*, 463:114949, 2019.

[29] Pålsson BA. A parameterized turnout model for simulation of dynamic vehicle–turnout interaction with an application to crossing geometry assessment. *In: Klomp M, Bruzelius F, Nielsen J, et al., editors. Advances in dynamics of vehicles on roads and tracks. IAVSD 2019 Cham:Springer; (Lecture Notes in Mechanical Engineering)*, 2020.

[30] Milošević MDG, Pålsson BA, Nissen A, Nielsen JCO, and Johansson H. Reconstruction of sleeper displacements from measured accelerations for model-based condition monitoring of railway crossing panels. *Mechanical Systems and Signal Processing*, 192:110225, 2023.

[31] Skrypnyk R, Ossberger U, Pålsson BA, Ekh M, and Nielsen JCO. Long-term rail profile damage in a railway crossing: Field measurements and numerical simulations. *Wear*, 472-473:203331, 2021.

[32] Craig RR and Bampton MCC. Coupling of substructures for dynamic analyses. *AIAA Journal*, 6(7):1313–1319, 1968.

[33] Iwnicki S. Manchester benchmarks for rail vehicle simulation. *Vehicle System Dynamics*, 30(3-4):295–313, 1998.

[34] A. Olsson, G. Sandberg, and O. Dahlblom. On Latin hypercube sampling for structural reliability analysis. *Structural Safety*, 25(1):47–68, 2003.

[35] Meyer J-E, Eriksson C, and Holmberg M. UHtsv. Spårväxel – Teknisk specifikation spårväxeltyp 60E, standard rörande trafikverkets spårväxlar (Turnout - Technical specification turnout type 60E, standard regarding turnouts of the Swedish Transport Administration, in Swedish), ctm 199 106, 2019. 29 pp.

[36] Nasrollahi K, Ramos A, Nielsen JCO, Dijkstra J, and Ekh M. Benchmark of calibrated 2D and 3D track models for simulation of differential settlement in a transition zone using field measurement data. *Engineering Structures*, 316:118555, 2024.